Cours du 5 décembre 2011

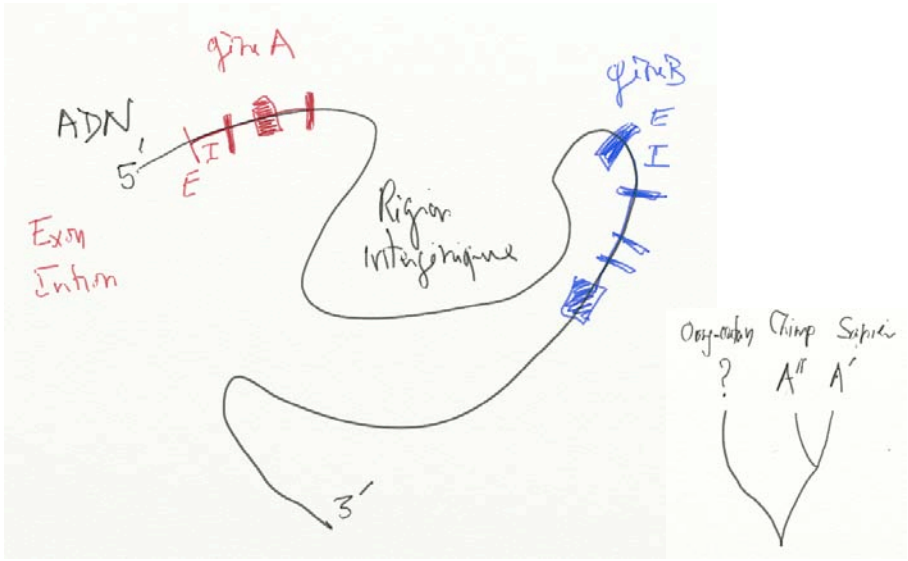

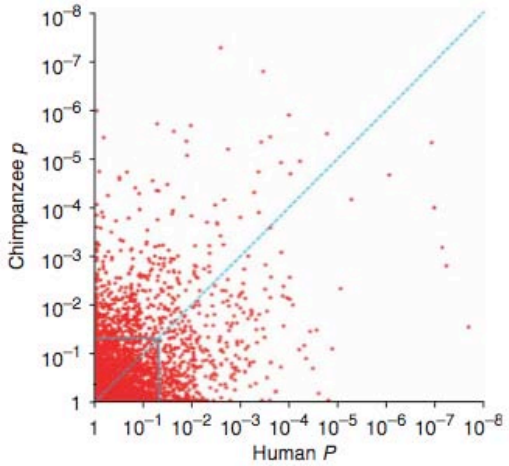

Figure 2 Positive selection in chimpanzees versus humans. Each point represents one gene; the *x*-axis represents *P* values on the human lineage, and the *y*-axis represents *P* values on the chimpanzee lineage. The solid blue lines correspond to *P* values of 0.05, and the dashed blue line corresponds to equal *P* values on the two lineages. Thus, genes scoring high in humans are plotted toward the lower right, genes scoring high in chimpanzees are plotted toward the upper left and genes scoring high in both species are plotted toward the center. (Several genes have $P < 10^{-8}$ on one lineage or the other and hence are not plotted.)

Promoter regions of many neural- and nutrition-related genes have experienced positive selection during human evolution

Nat Genet
2007 vol. 39 (9) pp. 1140-4

Haygood R, Fedrigo O, Hanson B, Yokoyama K, Wray G

Table 1 PANTHER biological process categories enriched for positive selection[a]

(a) Humans

Category[b]	Number of genes analyzed	Human P_{MW} [c]	Chimpanzee P_{MW} [c]
Protein folding	70	0.0067	0.77
Other neuronal activity[d]	31	0.013	0.039
Neurogenesis[e]	133	0.013	0.032
Glycolysis[f]	21	0.014	0.72
Neuronal activities[d]	137	0.020	0.22
Carbohydrate metabolism[f]	210	0.020	0.017
Ectoderm development[e]	169	0.020	0.11
Mesoderm development	161	0.024	0.17
Nerve–nerve synaptic transmission[d]	25	0.025	0.34
Vision	64	0.025	0.15
Oncogene	23	0.045	0.46
Anion transport	31	0.049	0.17

(b) Chimpanzees

Category[b]	Number of genes analyzed	Chimpanzee P_{MW} [c]	Human P_{MW} [c]
DNA replication	34	0.013	0.41
Carbohydrate metabolism[g]	210	0.017	0.020
Transport	414	0.029	0.50
Neurogenesis	133	0.032	0.013
Other neuronal activity	31	0.039	0.013
Other polysaccharide metabolism[g]	44	0.041	0.43
Blood clotting	32	0.049	0.47

[a]See **Supplementary Table 6** for further analyses. [b]Ordered by human (**a**) or chimpanzee (**b**) P_{MW}. Each listed category contains at least 20 analyzed genes. There are 127 such categories, with extensive overlap. [c]Nominal one-tailed Mann–Whitney *P* value: the probability that analyzed genes within the category have *P* values for positive selection no lower than analyzed genes outside the category. [d]The nerve-nerve synaptic transmission and other neuronal activity categories are contained in the neuronal activities category. For the remainder of the neuronal activities category, human $P_{MW} = 0.46$, and chimpanzee $P_{MW} = 0.62$. [e]The neurogenesis category is contained in the ectoderm development category. For the remainder of the ectoderm development category, human $P_{MW} = 0.44$ and chimpanzee $P_{MW} = 0.81$. [f]The glycolysis category is contained in the carbohydrate metabolism category. For the remainder of the carbohydrate metabolism category, human $P_{MW} = 0.080$ and chimpanzee $P_{MW} = 0.0078$. [g]The other polysaccharide metabolism category is contained in the carbohydrate metabolism category. For the remainder of the carbohydrate metabolism category, chimpanzee $P_{MW} = 0.073$ and human $P_{MW} = 0.014$.

Gènes neuraux

PRSS12	Apprentissage, mémorisation, retard mental
NTRK2	Récepteurs aux BDNF, obésité, "mood desorders"
UCHL3	Deubiquitinylation, mémoire de travail ?
STX1A	Syntaxine 1A, Transmission 5HT, Autisme
SCN1A	Canal sodique voltage dépendant, épilepsies
ISL2	Facteur de transcription, guidage axonal
SLIT2	Protéine sécrétée, guidage axonal
CHRNA9	Canal calcique, dépression bipolaire
ADAM22	Metalloprotease inactive, ligan des intégrines, adhésion, prolifération
SCN9A	Canal sodique, douleur d'origines inflammatoire
GLRA1	Récepteur à la glycine, contrôle du mouvement (spinal)
SCRG1	Protéine membranaire, Creutzfeld-Jakob
TMED10	Protéine membranaire, Alzheimer
ITM2C	Protéine membranaire, Alzheimer

Gènes métaboliques

ME2	Malate à Pyruvate
HK1	Hexokinase, première étape de la glycolyse
GCK	Glucokinase, première étape de la glycolyse
GPI	Glucose-6-Phosphate isomérase, deuxième étape de la glycolyse
PFKFB3	Modifie l'activité phosphofructokinase, troisième étape de la glycolyse
GCG	Glucagon-like peptide, Diabète trype 2
GALE	UDP-galactose 4 epimerase, cataracte juvénile, surdité, retard mental
KLF11	Facteur de transcription induit par le glucose, expression de l'Insuline
ABCC8	Canal potassique, sécrétion insuline
FOXC2	facteur de transcription, métabolisme des adipocytes, angiogenèse
LDHA	Conversion lactate-pyruvate
MMP20	Métalloprotéase, fabrication de l'émail
KRT4	Kératine, tube digestif (œsophage)
HSD17B4	Catabolisme des acides gras, peroxysomes, surdité, ataxie de Perrault, retard mental
MCEE	MethylmalonylCoA epimerase
USHBP1	Usher syndrome 1C binding protein 1, surdité, rétinopathie
HPD	4-hydroxyphenylpyruvate dioxygenase, retard mental, déséquilibres, épilepsie
SCLY	Selenocysteine lyase

Metabolic changes in schizophrenia and human brain evolution

Genome Biol
2008 vol. 9 (8) pp. R124

Khaitovich P, Lockstone H, Wayland M, Tsang T, Jayatilaka S, Guo A, Zhou J, Somel M, Harris L, Holmes E, Pääbo S, Bahn S

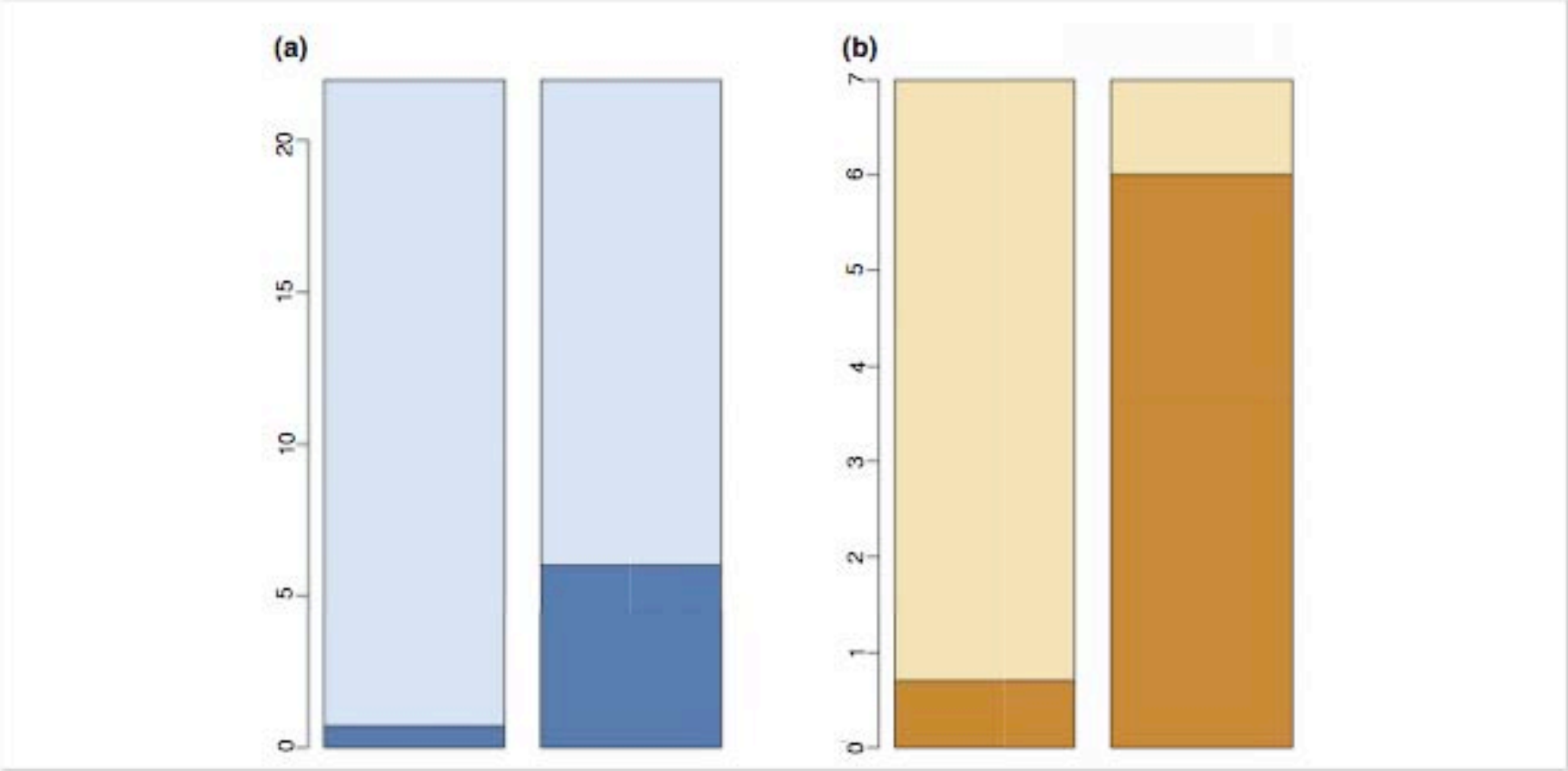

Figure 1
The proportion of biological processes showing evidence of recent positive selection on the human lineage that is differentially expressed in schizophrenia. The height of the bar represents the number of GO groups showing evidence of recent positive selection on the human lineage; **(a)** all 22 and **(b)** the 7 relating to energy metabolism. The darker shade of color represents the number of GO groups differentially expressed in schizophrenia among the 22 or the 7 GO groups (Wilcoxon rank sum test, $p < 0.03$, FDR = 11%). Left bar, expected by chance; right bar, observed.

Metabolic changes in schizophrenia and human brain evolution

Genome Biol
2008 vol. 9 (8) pp. R124

Khaitovich P, Lockstone H, Wayland M, Tsang T, Jayatilaka S, Guo A, Zhou J, Somel M, Harris L, Holmes E, Pääbo S, Bahn S

Detected metabolites and metabolite groups

Metabolite group	Number of peaks*	*t*-test *p*-value†	Effect size‡		
			H_{sch}/H_c	H_c/C	H_c/R
Creatine	2	0.000	2.3	-2.3	-4.9
Lactate	6	0.005	1.5	-2.7	-0.6
Phosphocholine	1	0.034	1.0	-1.4	-0.3
Glycerophosphocholine	1	0.042	1.0	-1.5	-0.7
N-acetylaspartate	5	0.040	0.9	-2.2	-1.8
Acetate	1	0.025	-1.1	-0.3	0.1
Glycine	1	0.024	-1.1	3.3	4.2
Choline	1	0.010	-1.4	4.0	3.4
Unknown§	6	0.002	-1.5	2.8	6.2
Taurine	3	0.080			
Glutamate/glutamine 1§¶	4	0.114			
Glutamate/glutamine 2¶	4	0.130			
Glutamine§	4	0.280			
Glutamate 1§¶	3	0.381			
Scyllo-inositol	1	0.404			
Gamma-aminobutyric acid	5	0.470			
Myo-inositol	9	0.630			
Glutamate/proline	1	0.710			
Myo-inositol/taurine	3	0.797			
Glutamate 2¶	5	0.841			
N-acetylaspartylglutamate	1	0.845			

*Number of peaks in the NMR spectrum corresponding to the metabolite/metabolite group. †Comparison between metabolite concentrations in 10 human schizophrenia patients and 12 human control individuals. ‡Effect size was calculated as the difference between means of metabolite concentrations between the groups normalized to the average standard deviation within the group. Positive values indicate higher concentration in group one, negative values higher concentration in group two. H_c, human controls; H_{sch}, human schizophrenia patients; C, chimpanzees; R, rhesus macaques. §These peaks show a high degree of spectral overlap with other unidentified baseline peaks. ¶Glutamine/glutamate and glutamate peaks were separated into two independent groups based on the intensity correlation analysis (see Materials and methods).

Metabolic changes in schizophrenia and human brain evolution

Genome Biol
2008 vol. 9 (8) pp. R124

Khaitovich P, Lockstone H, Wayland M, Tsang T, Jayatilaka S, Guo A, Zhou J, Somel M, Harris L, Holmes E, Pääbo S, Bahn S

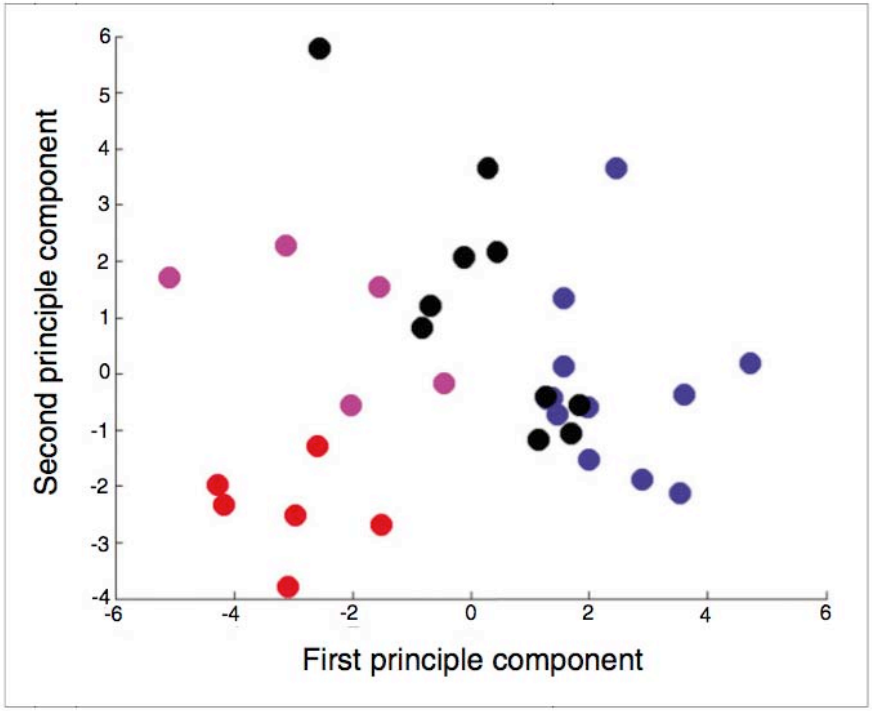

Figure 2
Principal component analysis of the metabolite abundance profiles in 33 individuals. The analysis is based on 21 detected metabolites. Each point represents an individual. The colors indicate: blue, human controls; black, human schizophrenia patients; purple, chimpanzees; red, rhesus macaques.

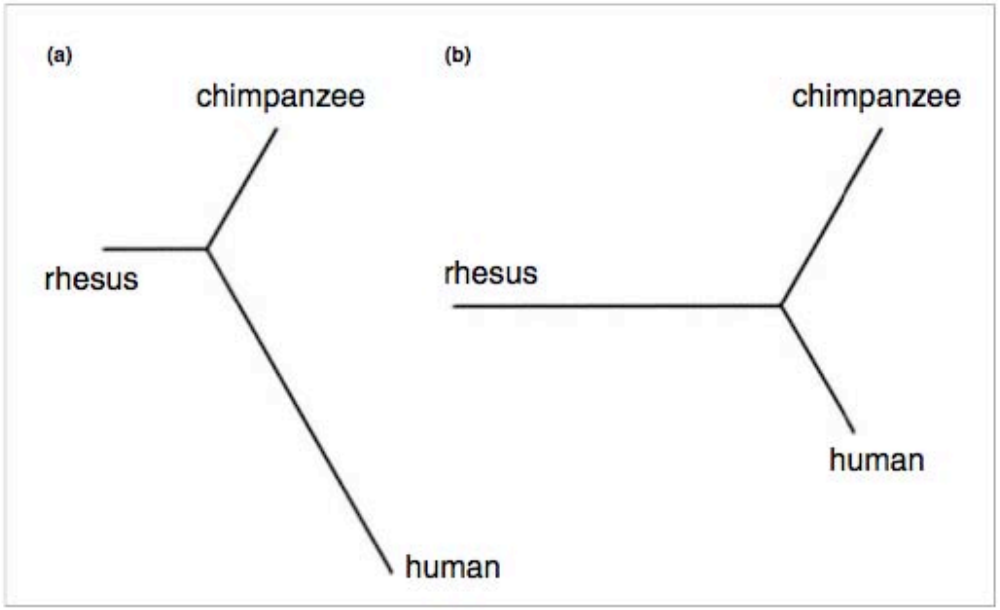

Figure 3
Divergence in metabolite abundance on the human and chimpanzee lineages. The trees are based on the abundance measurements of **(a)** 9 metabolites with significant concentration difference between human controls and schizophrenia patients and **(b)** 12 metabolites with no difference between these two groups. The trees were built using a neighbor-joining algorithm.

Rapid metabolic evolution in human prefrontal cortex

Fu X, Giavalisco P, Liu X, Catchpole G, Fu N, Ning ZB, Guo S, Yan Z, Somel M, Pääbo S, Zeng R, Willmitzer L, Khaitovich P

Proc Natl Acad Sci USA
2011 vol. 108 (15) pp. 6181-6

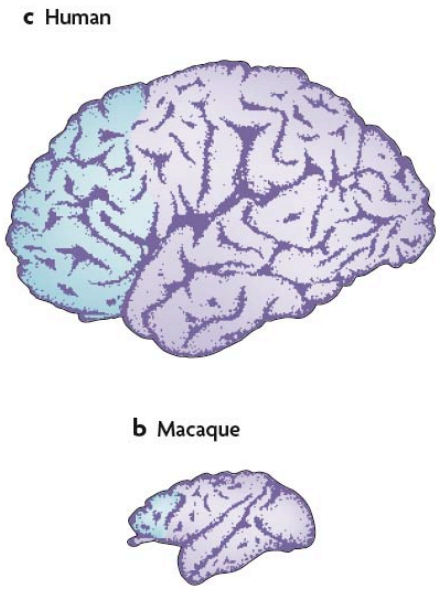

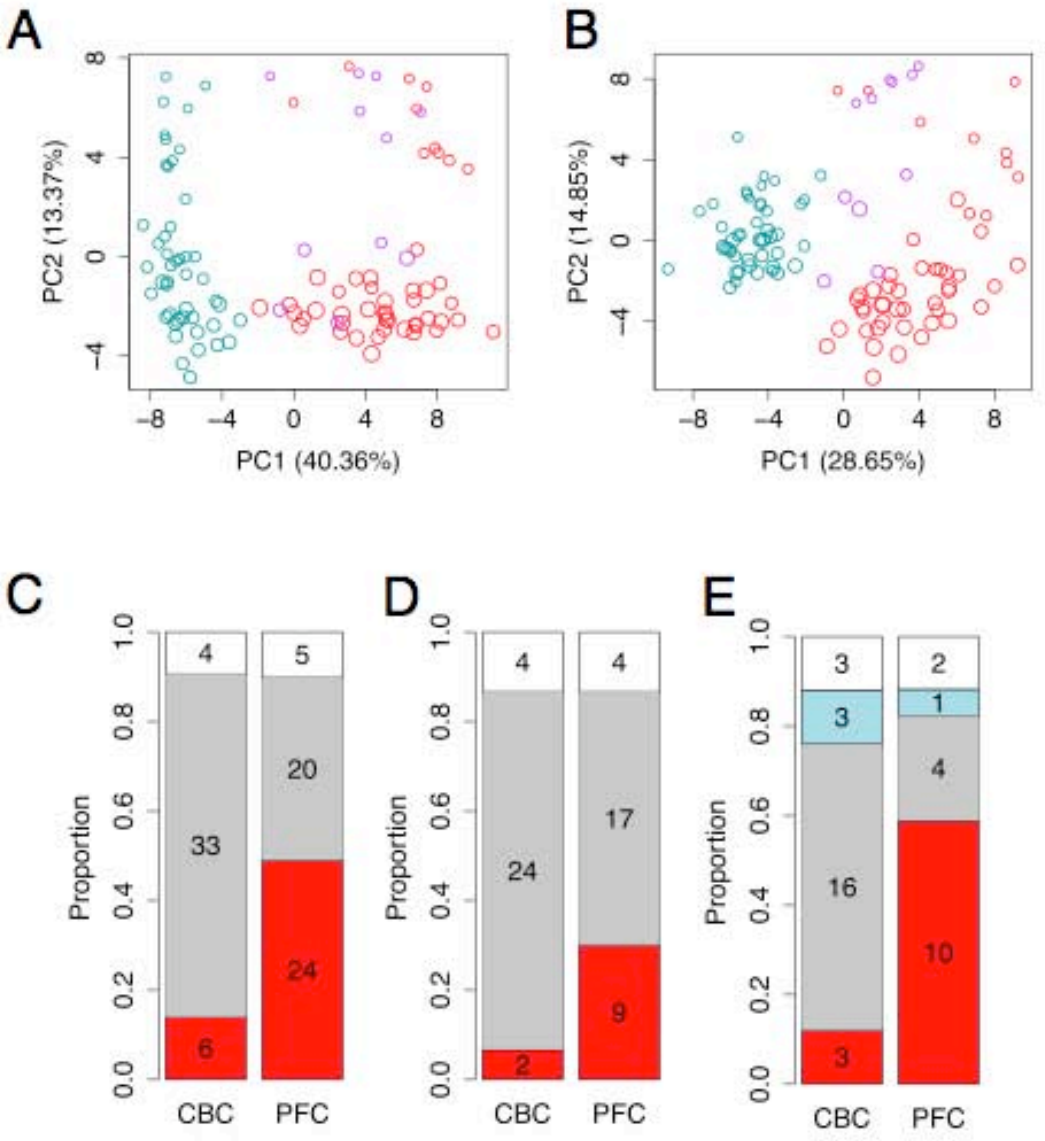

Fig. 1. Metabolite variation among species. (*A* and *B*) Principal component analysis of CBC and PFC metabolomes of the three species based on 92 detected metabolites. Each circle represents an individual. Size of circles is proportional to the individuals' ages, with larger circles corresponding to older individuals. Colors represent species: red, human; purple, chimpanzee; blue, rhesus macaque. (*C*–*E*) Proportions of human-specific (red), macaque-specific (gray), chimpanzee-specific (blue), and uncategorized metabolites (white) among the following: (*C*) the 43 and 49 metabolites with significant difference in concentration profiles between humans and rhesus macaques in CBC and PFC, respectively, identified using the full set of individuals; (*D*) the 30 metabolites with significant difference in concentration profiles between humans and rhesus macaques in both CBC and PFC; (*E*) the 25 and 17 metabolites with significant difference in concentration profiles among humans, chimpanzees, and rhesus macaques identified in CBC and PFC, respectively, using the subsets of 11 individuals per species matched using stage-of-life approach (*SI Appendix*). Numbers indicate numbers of metabolites in corresponding category. (*F* and *G*) Hierarchical clustering based on concentration profiles of 24 metabolites classified as human specific in PFC and six metabolites classified as human specific in CBC. Column headers indicate species: Ch, chimpanzee; Hu, human; Ma, rhesus macaque. Red and blue color intensities indicate metabolite concentration levels at different age normalized to mean equal a value of 0 and SD equal a value of 1 within each brain region.

Rapid metabolic evolution in human prefrontal cortex

Fu X, Giavalisco P, Liu X, Catchpole G, Fu N, Ning ZB, Guo S, Yan Z, Somel M, Pääbo S, Zeng R, Willmitzer L, Khaitovich P

Proc Natl Acad Sci USA
2011 vol. 108 (15) pp. 6181-6

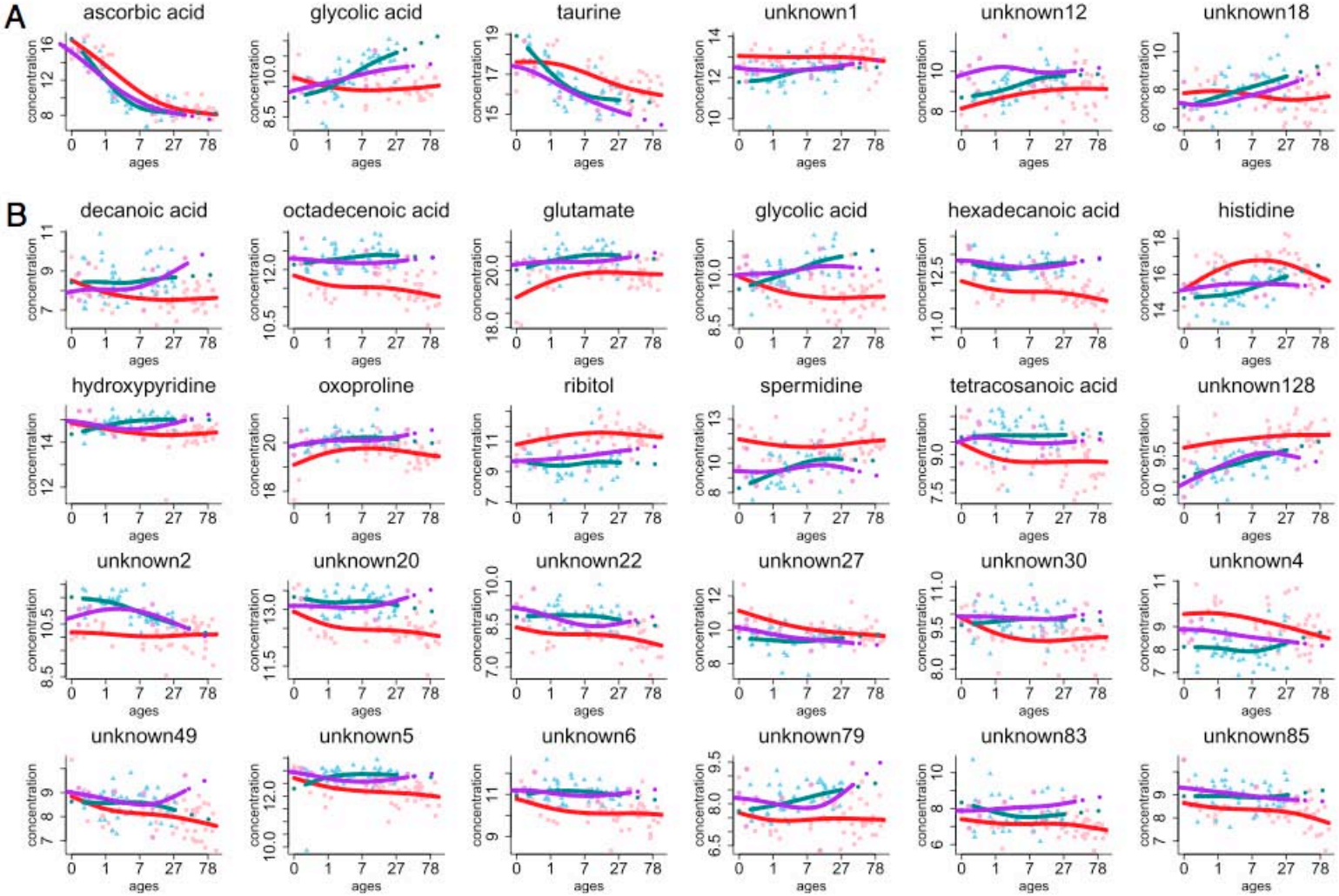

Fig. 2. Metabolites with human-specific concentration profiles. Shown are the six metabolites with human-specific concentration profiles in CBC (*A*) and 24 metabolites with human-specific concentration profiles in PFC (*B*). Points show metabolite concentrations in each individual. Colors represent species: red, humans; purple, chimpanzees; and blue, rhesus macaques. Lines are spline curves fitted to data points with 3 df. The *x* axis shows individuals' ages in years. The *y* axis shows normalized GC-MS measurements representing metabolite concentrations. Titles show metabolite annotation. Unannotated metabolites are labeled "unknown."

Cellular scaling rules for primate brains

Proc Natl Acad Sci USA
2007 vol. 104 (9) pp. 3562–7

Herculano-Houzel S, Collins CE, Wong P, Kaas JH

Table 1. Comparative cellular composition of the brain of the tree shrew and six primate species

Species	Body mass, g	Brain mass, g	Total neurons, $\times 10^6$	Total nonneurons, $\times 10^6$
Tree shrew	172.5 ± 3.5	2.752 ± 0.011	261.40	199.65
Marmoset	361.0 ± 1.4	7.780 ± 0.654	635.80 ± 115.73	590.74 ± 70.81
Galago	946.7 ± 102.6	10.150 ± 0.060	936.00 ± 115.36	666.59 ± 63.50
Owl monkey	925.0 ± 35.4	15.730	1,468.41	1,195.13
Squirrel monkey	n.a.	30.216	3,246.43	2,075.03
Capuchin monkey	3,340.0	52.208	3,690.52	3,297.74
Macaque monkey	3,900.0	87.346	6,376.16	7,162.90
Variation, macaque/marmoset	10.8×	11.2×	10.0×	12.1×

Species ordered by increasing brain size. Values are mean ± SD. n.a., not available.

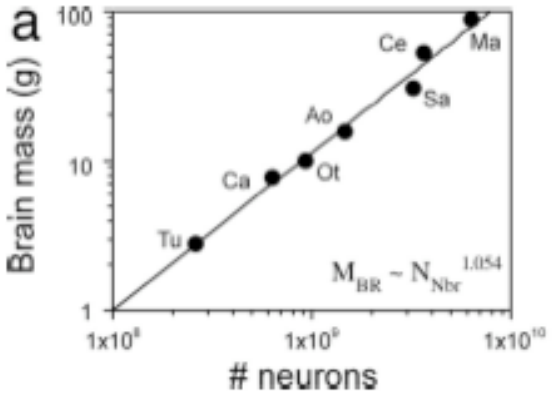

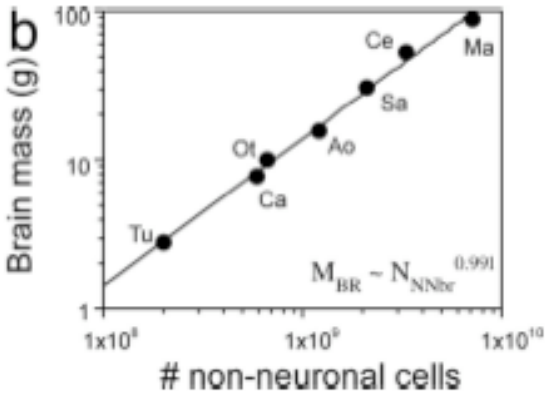

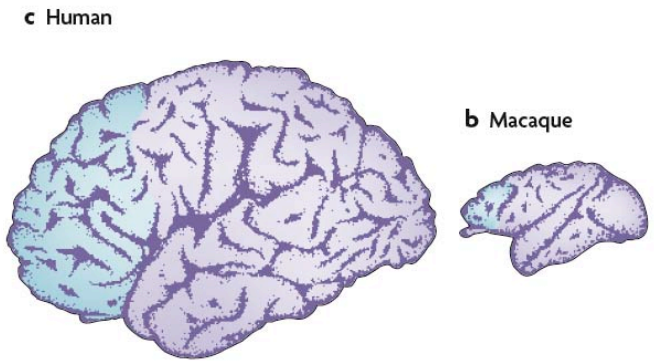

Evolution of increased glia–neuron ratios in the human frontal cortex

Proc Natl Acad Sci USA
2006 vol. 103 (37) pp. 13606–11

Sherwood CC, Stimpson CD, Raghanti MA, Wildman DE, Uddin M, Grossman LI, Goodman M, Redmond JC, Bonar CJ, Erwin JM, Hof PR

Table 2. Glia–neuron ratios in layer II/III of different areas in frontal cortex

Species	*n*	Area 4	Area 9L	Area 32	Area 44
Homo sapiens	6	2.19 (0.06)	1.65 (0.09)	1.63 (0.09)	1.55 (0.18)
Pan troglodytes	6	1.54 (0.05)	1.20 (0.06)	0.91 (0.09)	1.24 (0.13)
Macaca maura	6	1.29 (0.09)	0.84 (0.03)	0.68 (0.05)	0.95 (0.06)

Data are presented as mean (standard error).

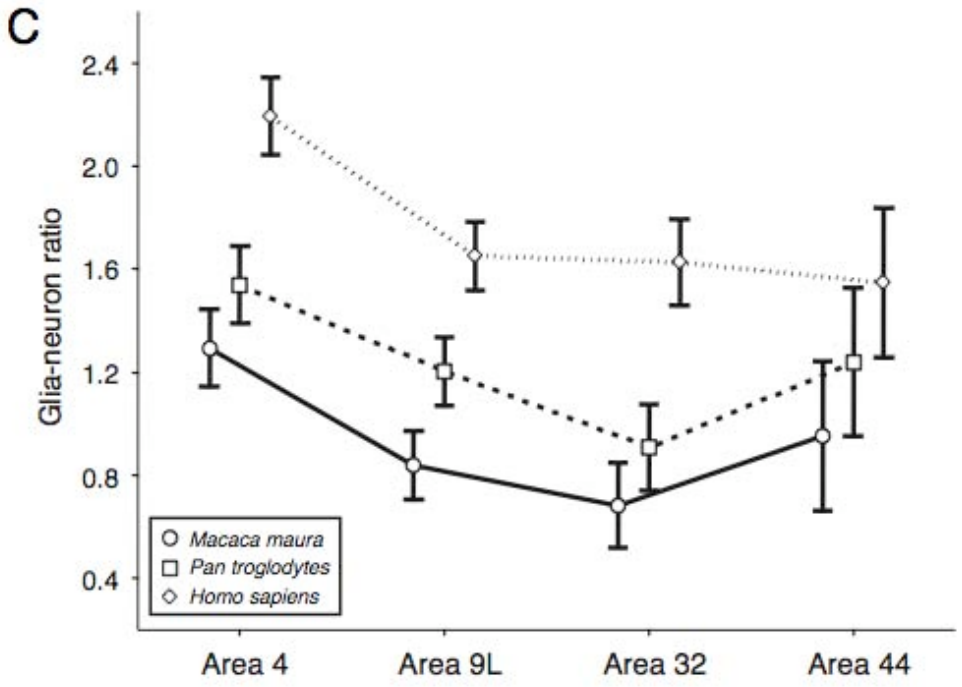

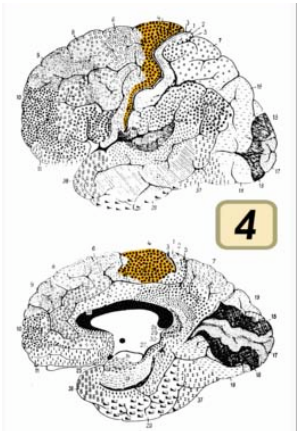

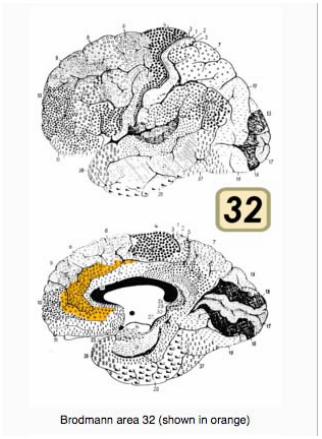

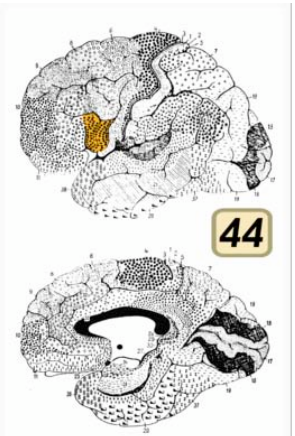

Evolution of increased glia–neuron ratios in the human frontal cortex

Proc Natl Acad Sci USA
2006 vol. 103 (37) pp. 13606–11

Sherwood CC, Stimpson CD, Raghanti MA, Wildman DE, Uddin M, Grossman LI, Goodman M, Redmond JC, Bonar CJ, Erwin JM, Hof PR

Table 1. Brain weights and glia–neuron ratios for layer II/III of prefrontal area 9L (species mean)

Species	*n*	Brain weight, g	Glia–neuron ratio
Homo sapiens	6	1,373.3	1.65
Pan troglodytes	6	336.2	1.20
Gorilla gorilla	2	509.2	1.21
Pongo pygmaeus	2	342.7	0.98
Hylobates muelleri	1	101.8	1.22
Papio anubis	2	155.8	0.97
Mandrillus sphinx	1	159.2	1.02
Macaca maura	6	92.6	0.84
Erythrocebus patas	2	102.3	1.09
Cercopithecus kandti	1	71.6	1.15
Colobus angolensis	1	74.4	1.20
Trachypithecus francoisi	1	91.2	1.14
Alouatta caraya	1	55.8	1.12
Saimiri boliviensis	1	24.1	0.51
Aotus trivirgatus	1	13.2	0.63
Saguinus oedipus	1	10.0	0.46
Leontopithecus rosalia	2	12.2	0.60
Pithecia pithecia	1	30.0	0.64

Linking neurodevelopmental and synaptic theories of mental illness through DISC1

Nat Rev Neurosci
2011 vol. 12 (12) pp. 707-22

Brandon NJ, Sawa A

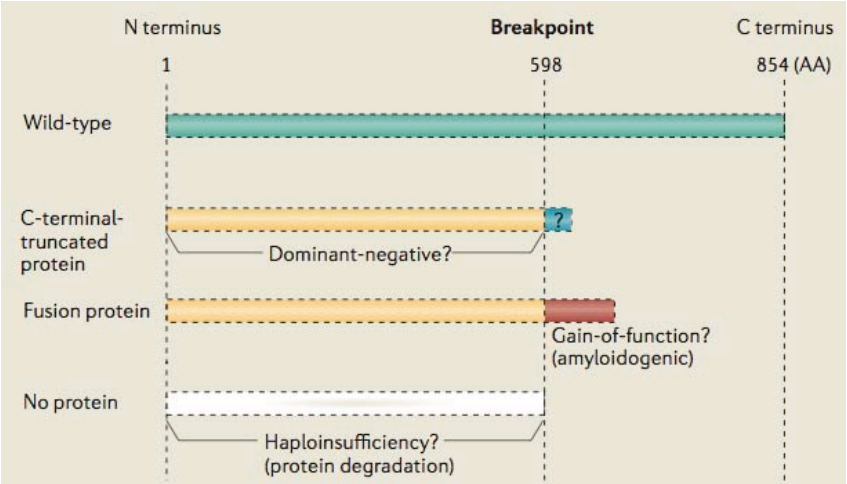

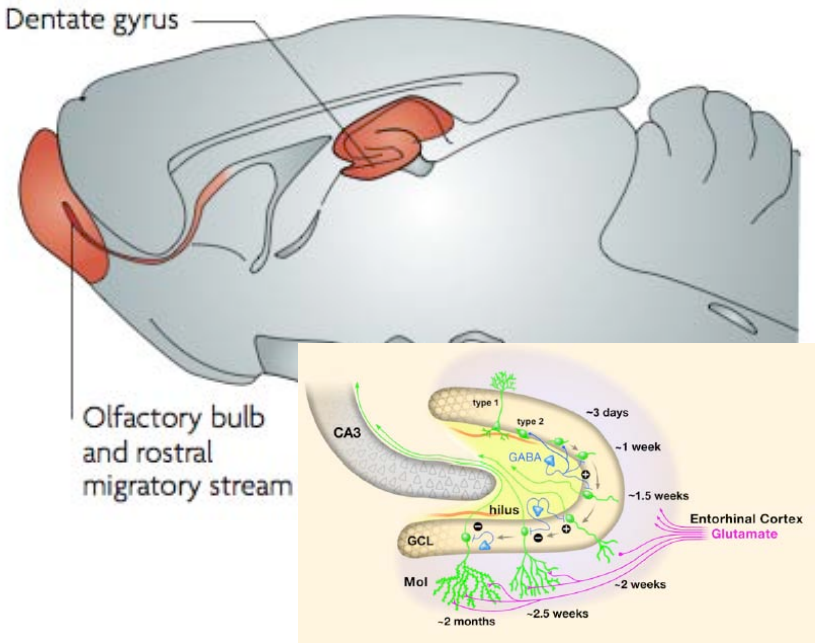

Disrupted-In-Schizophrenia 1 regulates integration of newly generated neurons in the adult brain

Cell
2007 vol. 130 (6) pp. 1146-58

Duan X, Chang JH, Ge S, Faulkner RL, Kim JY, Kitabatake Y, Liu XB, Yang CH, Jordan JD, Ma DK, Liu CY, Ganesan S, Cheng HJ, Ming G, Lu B, Song H

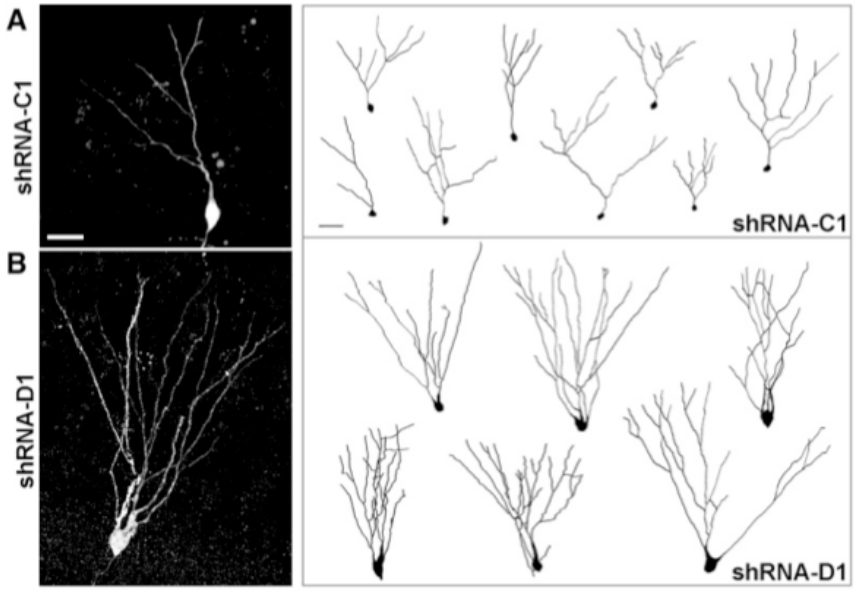

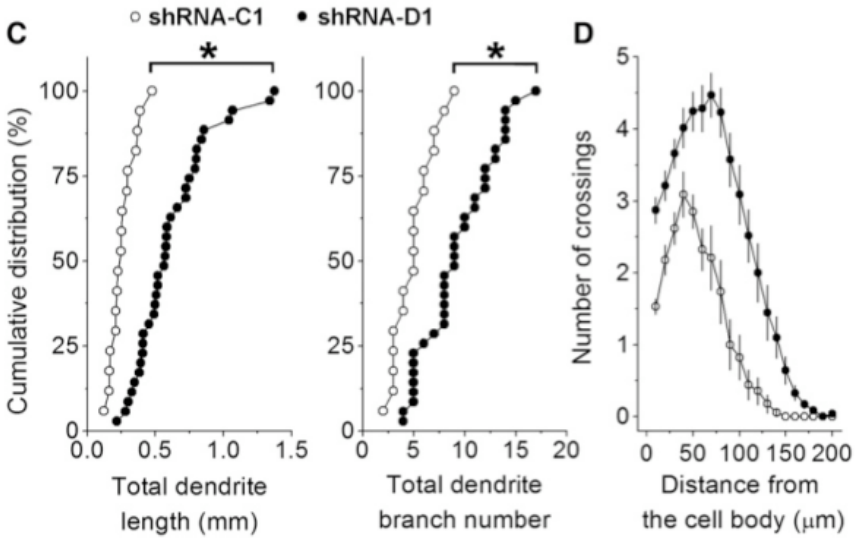

Linking neurodevelopmental and synaptic theories of mental illness through DISC1

Nat Rev Neurosci
2011 vol. 12 (12) pp. 707–22

Brandon NJ, Sawa A

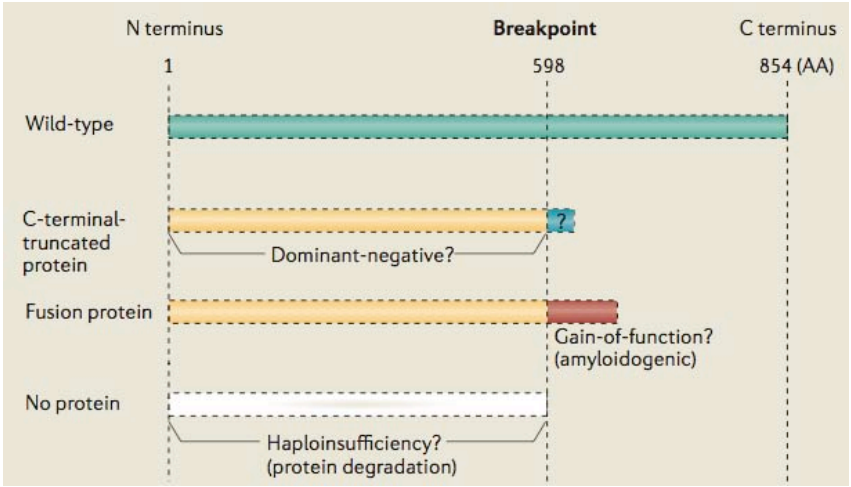

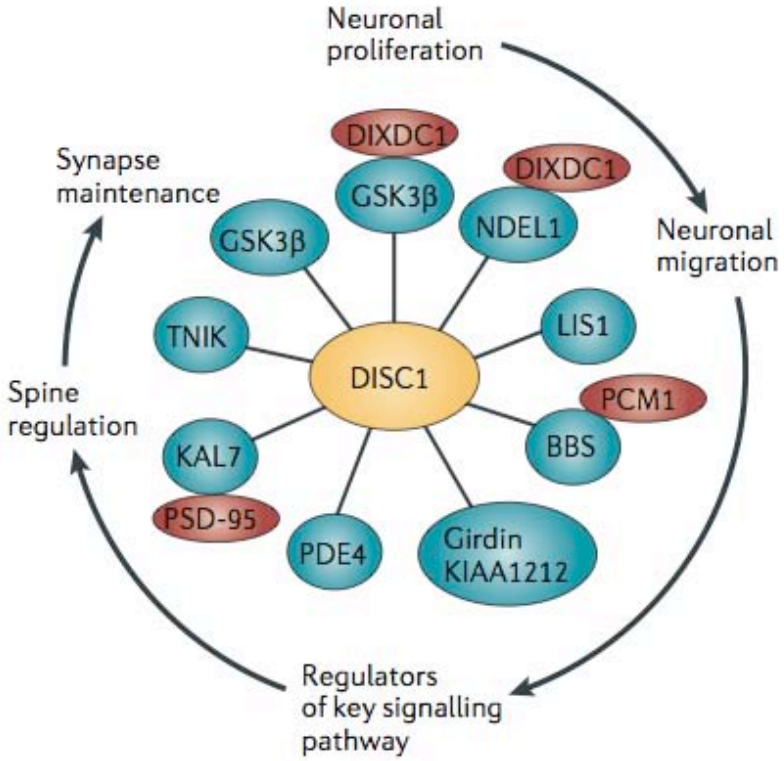

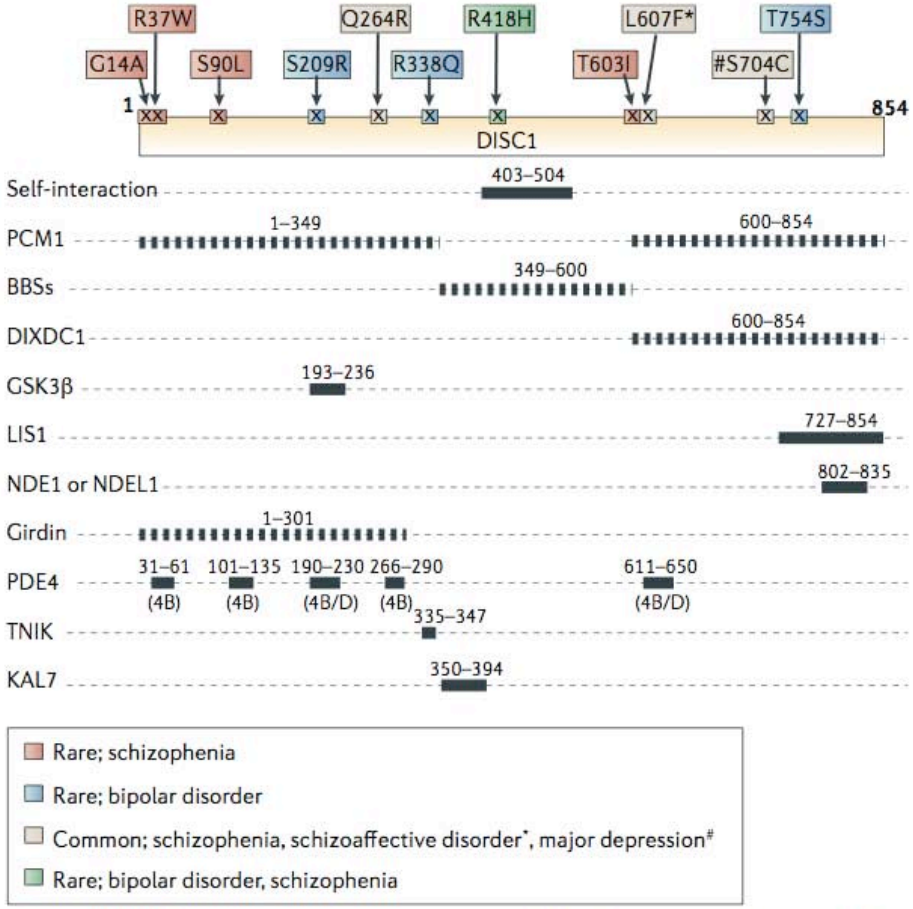

Figure 2 | **DISC1 protein interaction domains and relationship to the location of rare human variants associated with mental disorders.** Diagram of protein–protein interaction domains mapped onto disrupted in schizophrenia 1 (DISC1) and key DISC1 genetic variants (top) possibly associated with mental disorders[34–38,78,82,87,90,95,110,111,141,185,200]. Genetic variants at Q264R, L607F and S704C (common variants) are associated with schizophrenia. Furthermore, associations with L607F (indicated by *) and S704C (indicated by #) are reported for schizoaffective disorder and major depression, respectively. Please note that the binding sites have been mapped using a range of different approaches, so the resolution achieved in individual interactions is different (dotted lines are sites awaiting fine mapping). The self-interaction site refers to the domain through which DISC1 binds to itself. PCM1, pericentriolar material 1; BBS, Bardet–Biedl syndrome; DIXDC1, DIX domain containing 1; GSK3β, glycogen synthase kinase 3β; KAL7, kalirin 7; LIS1, lissencephaly protein 1; NDE1, nuclear distribution protein nudE homologue 1; NDEL1, nuclear distribution protein nudE-like 1; PDE4, phosphodiesterase type 4; TNIK, TRAF2- and NCK-interacting protein kinase.

Mitochondria in Neuroplasticity and Neurological Disorders

748 Neuron 60, December 11, 2008 ©2008 Elsevier Inc.

Mark P. Mattson,[1,*] Marc Gleichmann,[1] and Aiwu Cheng[1]

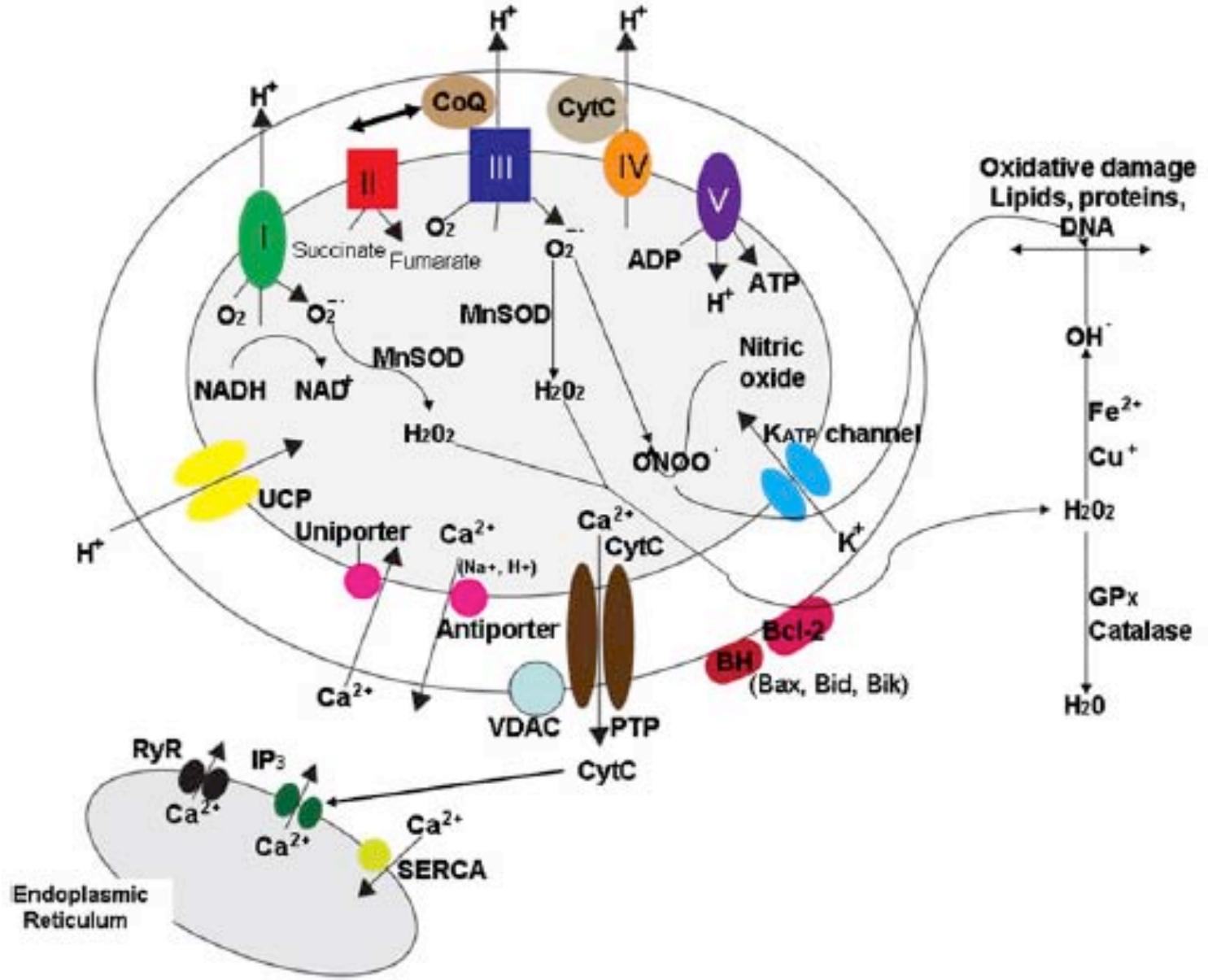

Disrupted-in-schizophrenia 1 (DISC1) plays essential roles in mitochondria in collaboration with Mitofilin

Proc Natl Acad Sci USA
2010 vol. 107 (41) pp. 17785-90

Park YU, Jeong J, Lee H, Mun JY, Kim JH, Lee JS, Nguyen MD, Han SS, Suh PG, Park SK

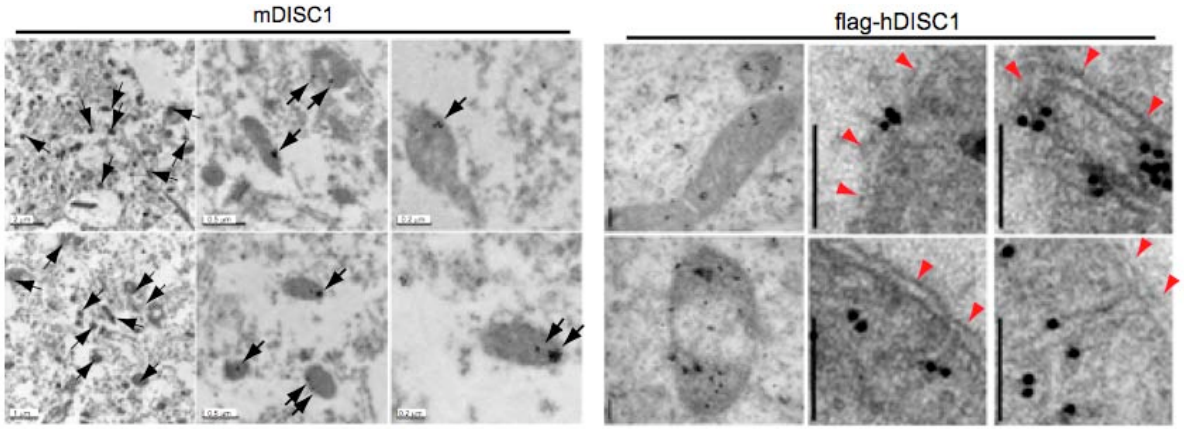

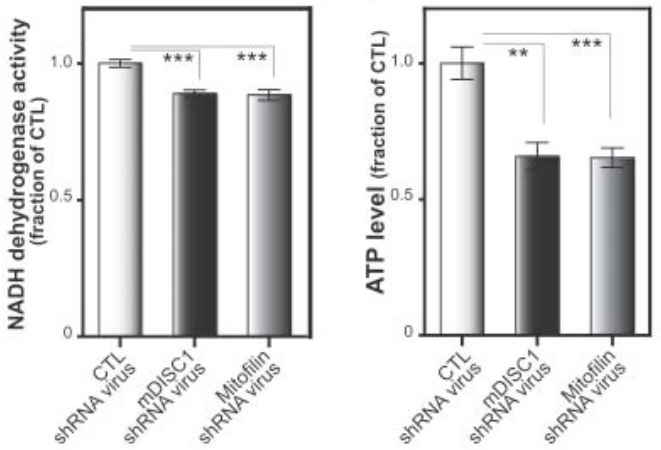

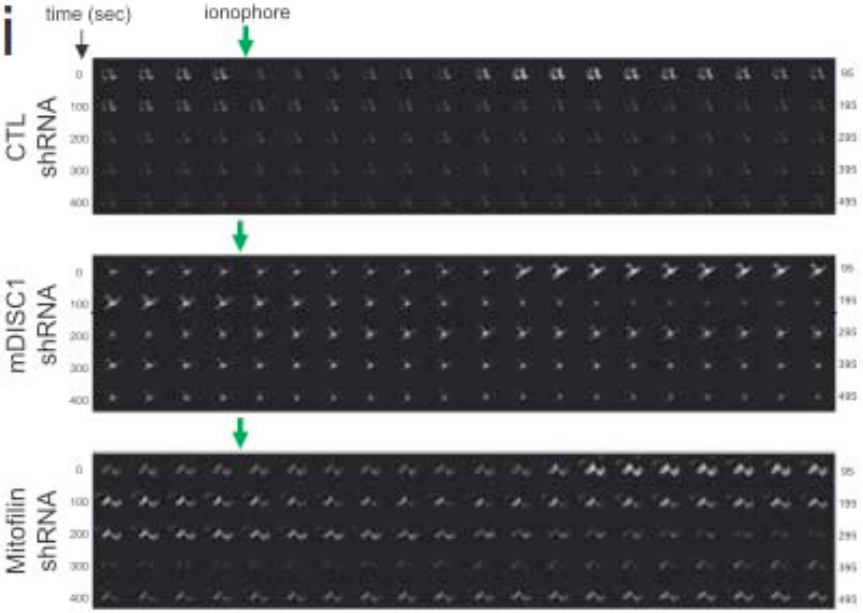

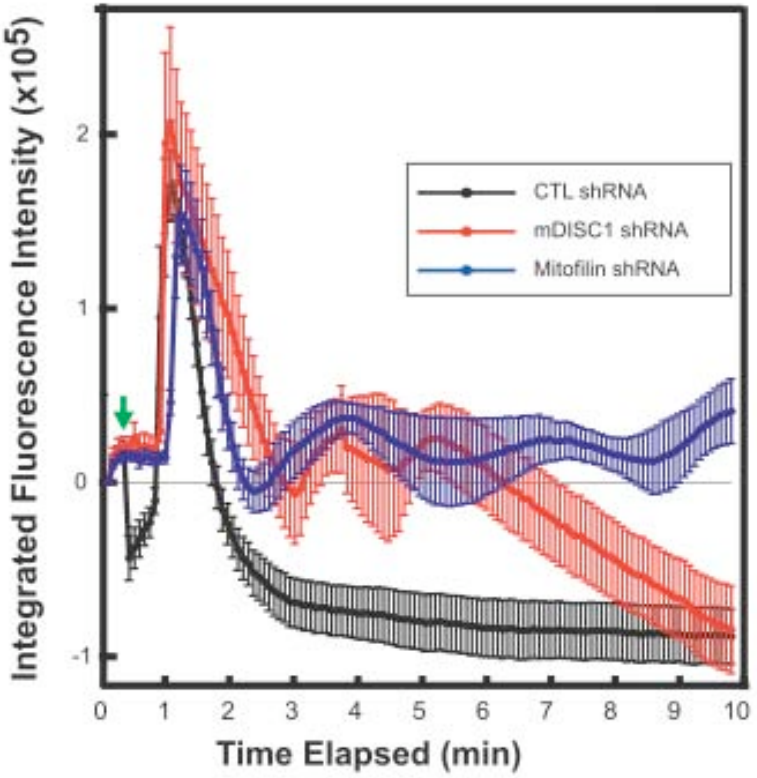

Disrupted in Schizophrenia-1 regulates intracellular trafficking of mitochondria in neurons

Molecular Psychiatry
2011 vol. 16 (2) pp. 122-4, 121

Atkin TA, Macaskill AF, Brandon NJ, Kittler JT